

Self-Association of Cholesterol-End-Capped Poly(sodium 2-(acrylamido)-2-methylpropanesulfonate) in Aqueous Solution

Shin-ichi Yusa,[†] Mikiharu Kamachi,[‡] and Yotaro Morishima^{*,§}

Department of Applied Chemistry, Himeji Institute of Technology, 2167 Shosha, Himeji 671-2201, Japan; Department of Applied Physics and Chemistry, Fukui University of Technology, 6-3-1 Gakuen Fukui 910-0028, Japan; and Department of Macromolecular Science, Graduate School of Science, Osaka University, Toyonaka, Osaka 560-0043, Japan

Received May 21, 1999; Revised Manuscript Received November 8, 1999

ABSTRACT: Poly(2-(acrylamido)-2-methylpropanesulfonic acid) sodium salt end-capped with a cholesterol moiety (Chol-PAMPS) was prepared by free radical polymerization of 2-(acrylamido)-2-methylpropanesulfonic acid (AMPS) initiated by a cholesterol-substituted azo compound, 4,4'-azobis(4-cyano-1-cholesteryl)pentanoate, and the associative behavior of Chol-PAMPS in aqueous solution was studied by ¹H NMR, size exclusion chromatography (SEC), static light scattering (SLS), quasielastic light scattering (QELS), and fluorescence probe techniques. For a reference polymer (AIBN-PAMPS), polyAMPS of a similar molecular weight with that of Chol-PAMPS was prepared in the presence of 2,2'-azobis(2-methylpropionitrile) as an initiator. The degree of polymerization (DP) of Chol-PAMPS was estimated to be about 70 from a ¹H NMR spectrum (in DMSO-*d*₆) by assuming disproportionation for the termination. This DP value agreed fairly well with that estimated by SEC in water/acetonitrile using sodium poly(styrenesulfonate)s as standards. QELS indicated that Chol-PAMPS formed multipolymer aggregates at polymer concentrations (*C*_p) higher than 0.5 g/L in 0.1 M NaCl. Fluorescence emission and excitation spectra for pyrene probes solubilized in the aggregates of Chol-PAMPS suggested the presence of a critical micelle concentration (cmc) around *C*_p ≈ 0.6 g/L in water. Above this *C*_p, the micellelike aggregates coexist with unimers over a wide range of *C*_p. In the *C*_p regime of 1.0–5.0 g/L, hydrodynamic radii for the aggregates were practically constant at about 50 nm. However, when *C*_p was increased beyond this *C*_p regime, the size increased considerably with *C*_p. Given DP ≈ 70 for Chol-PAMPS, these sizes for the aggregates are obviously too large for a single spherical micelle with cholesterol groups in the core and extended polyAMPS chains in the corona. The structures of these multipolymer aggregates remain to be an open question, but these results are explained by considering that some polymer chains possess cholesterol groups at both chain ends and spherical micelles are bridged by these polymer chains.

Introduction

Macromolecular self-association has received increasing interest of chemists during the past decade. In general, macromolecular self-associations are driven by noncovalent interactions including Coulombic, hydrogen bonding, van der Waals, exchange repulsive, and hydrophobic interactions. Among others, hydrophobic interactions are an important driving force for self-association of amphiphilic polymers in water. Therefore, a practical approach to the synthesis of self-assembling polymers is to covalently introduce some hydrophobes into water-soluble polymers. Hydrophobes can be incorporated into various parts of a polymer chain. A large number of hydrophobes can be attached to a polymer chain by copolymerization of hydrophilic and hydrophobic monomers with a block, alternating, or random distribution. A limited number of hydrophobes can be introduced into the side chains of water-soluble polymers by chemical reaction with use of polymers with reactive side chains and hydrophobic reagents. Furthermore, hydrophobic moieties can be attached at polymer chain ends.

It is well-known that sterols are widely present in membranes of most eukaryotic cells. Cholesterol (Chol) is one of the most common membrane sterols in animals

that regulates membrane fluidity.¹ In the presence of Chol, fluidity of membrane is reduced. This effect of Chol arises from the rigidity of the steroid ring system. Thus, Chol plays an important role in self-association of molecules in biological systems.

Akiyoshi et al.^{2–5} have reported that pullulan covalently incorporated with a few Chol per 100 glucose units forms stable nanoparticles upon interpolymer self-association in aqueous solution, Chol association acting as a cross-link for the hydrogel formation. In our previous work, we incorporated a small amount (≤5 mol %) of Chol into polyelectrolytes by random copolymerization of 2-(acrylamido)-2-methylpropanesulfonic acid (AMPS) sodium salt and cholesteryl 6-(methacryloyloxy)hexanoate.⁶ These Chol-containing amphiphilic polyelectrolytes form an intermolecularly bridged flower-type micelle in aqueous solution. These findings suggest that Chol has a strong tendency for self-association even if the contents of Chol in polymers are very low. This led us to anticipate that we could design strongly self-associative polymers by utilizing cholesteryl moieties in a very small amount.

Winnik and co-workers^{7,8} synthesized amphiphilic derivatives of poly(*N*-isopropylacrylamide) (PNIPAM) consisting of a PNIPAM chain substituted at one end with a dioctadecyl group by free radical polymerization of *N*-isopropylacrylamide using 4,4'-azobis(4-cyano-*N,N*-dioctadecyl)pentanamide as an initiator. In aqueous solution, the end-dioctadecylated PNIPAM forms a multimolecular core–corona type micelle under tem-

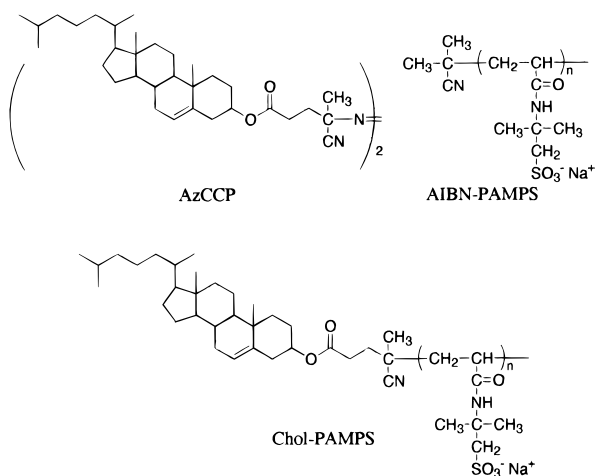
* To whom correspondence should be addressed.

[†] Himeji Institute of Technology.

[‡] Fukui University of Technology.

[§] Osaka University.

Chart 1



peratures below the lower critical solution temperature (LCST), the micelle consisting of a core of dioctadecyl chains and corona of solvated PNIPAM chains. Almgren et al.⁹ reported the aggregation behavior of hydrophobically end-capped poly(ethylene oxide) in aqueous solution. At very low concentrations, the polymers exist in the form of unimer, some of which are closed to loops, or in small oligomeric aggregates. In semidilute or concentrated regimes, micellelike polymer aggregates are formed. At higher concentrations, the polymer chains form infinite network.

These studies motivated us to synthesize amphiphilic polyAMPS substituted with a Chol moiety at a chain-end by applying the method developed by Winnik and co-workers.⁷ We synthesized a Chol-substituted azo initiator, 4,4'-azobis(4-cyano-1-cholesteryl)pentanoate (AzCCP), and performed free radical polymerization of AMPS using AzCCP as an initiator to obtain Chol-end-capped polyAMPS (Chol-PAMPS) (Chart 1). The association behavior of Chol-PAMPS in aqueous solution was investigated by ¹H NMR, size exclusion chromatography (SEC), static light scattering (SLS), quasielastic light scattering (QELS), and fluorescence techniques.

Experimental Section

Materials. 2-(Acrylamido)-2-methylpropanesulfonic acid (AMPS), purchased from Wako Pure Chemical Co., was used without further purification. Pyrene was purchased from Nacalai Tesque and purified by recrystallization from ethanol. 1,6-Diphenyl-1,3,5-hexatriene (DPH) was purchased from Nacalai Tesque and used without further purification. Water was purified with a Millipore Milli-Q System.

4,4'-Azobis(4-cyano-1-cholesteryl)pentanoate (AzCCP). A few drops of *N,N*-dimethylformamide (DMF) and 10 g (35.7 mmol) of 4,4'-azobis(4-cyanovaleric acid) were dissolved in 10 mL of thionyl chloride. The mixture was stirred for 2 h at 0 °C. Thionyl chloride was then removed under reduced pressure to give a solid product of 4,4'-azobis(4-cyanovaleryl chloride). The product was dissolved in 300 mL of dry tetrahydrofuran (THF), and the solution was added to a 50 mL of dry THF solution containing 28 g (0.07 mol) of cholesterol and 3.0 g (0.07 mol) of pyridine over a period of 30 min at 0 °C. After 6 h, the solvent was removed, and the crude product was dissolved in diethyl ether. The solution was washed with aqueous NaHCO₃ and dried over anhydrous Na₂SO₄. After the solvent was removed, the crude product was recrystallized from ether/methanol (1/1, v/v): yield 1.72 g (2.4%); mp 132–134 °C. ¹H NMR (CDCl₃): δ 0.6–2.6 (m, 100H), 4.5–4.7 (m, 2H), 5.4 (m, 2H). Anal. Calcd for C₆₆H₁₀₄O₄N₄: C, 77.90; H, 10.30; N, 5.51. Found: C, 77.61; H, 10.25; N, 5.49.

Cholesterol-End-Capped PolyAMPS (Chol-PAMPS).

To a 19.3 mL DMF solution containing 2.0 g (9.65 mmol) of AMPS and an equimolar of Na₂CO₃ was added 99.8 mg (0.097 mmol) of AzCCP. The solution was placed in a glass ampule and outgassed on a vacuum line by six freeze–pump–thaw cycles, and then the ampule was vacuum-sealed. Polymerization was carried out at 60 °C for 72 h. The polymer was purified by reprecipitating from methanol into a large excess of diethyl ether twice. The polymer was then dissolved in pure water, and the aqueous solution was dialyzed against pure water for a week. The polymer was recovered by freeze-drying (1.80 g, 81.3%).

Reference Polymer (AIBN–PAMPS). The polymerization was carried out with 2.0 g (9.65 mmol) of AMPS, an equimolar of Na₂CO₃, and 15.8 mg (0.097 mmol) of 2,2'-azobis(2-methylpropanitrile) (AIBN) in 19.3 mL of DMF at 60 °C for 72 h to yield 1.86 g of polymer (84.1%).

Measurements. a. ESR. Spectra were recorded on a JEOL model JES RE-2X ESR spectrometer with a JEOL ESPRIT 330 data processor. Sample solutions were degassed by purging with argon for 30 min.

b. ¹H NMR. Spectra were obtained with a JEOL EX-270 spectrometer using a deuterium lock at a constant temperature of 30 °C during the whole run.

c. Size Exclusion Chromatography (SEC). Analysis was performed at 45 °C with a TOSOH CCP & 8020 series equipped with an UV-8010 UV detector. A combined column of TSKgel G6000PW_{XL} and G3000PW_{XL} (TOSOH) was employed. For an eluent, 0.2 M phosphate buffer (pH = 7.0) containing 10% of acetonitrile was used. The polymer concentration in sample solutions was 0.5 g/L. Standard sodium poly(styrenesulfonate) samples were used to calibrate molecular weights.

d. Static Light Scattering (SLS). SLS data were obtained at 25 °C with an Otsuka Electronics Photol DLS-700 light scattering spectrometer equipped with an Ar laser (75 mW at 488 nm). Values of *dn/dc* (refractive index increment against concentration) were determined with an Otsuka DRM-1020 differential refractometer. Sample solutions were filtered with a 0.1 μm pore size membrane filter prior to measurement.

e. Quasielastic Light Scattering (QELS). QELS data were obtained at 25 °C with an Otsuka Electronics Photol DLS-700 light scattering spectrometer equipped with an ALV-5000 multi-τ digital time correlator. Polymer sample solutions were filtered with a 0.1 μm pore size membrane filter prior to measurement. The scattered light of an Ar laser (75 mW at 488 nm) was measured at scattering angles (θ) of 30, 50, 70, 90, 110, and 130°. The intensity autocorrelation function *g*⁽²⁾(*t*) was measured by QELS. The intensity autocorrelation function is related to the normalized autocorrelation function *g*⁽¹⁾(*t*), described as

$$g^{(2)}(t) = B[1 + \beta|g^{(1)}(t)|^2] \quad (1)$$

where β is a parameter of the optical system (constant) and *B* is a baseline. The inverse Laplace transform (ILT) analysis was performed using the algorithm REPES¹⁰ to obtain the relaxation time distribution, τ*A*(τ), according to

$$g^{(1)}(t) = \int \tau A(\tau) \exp(-t/\tau) d \ln \tau \quad (2)$$

where τ is the relaxation time. The relaxation rate, Γ = τ⁻¹, is a function of the polymer concentration and the scattering angle, θ.¹¹ The translational diffusion coefficient, *D*, could be calculated from *D* = Γ/*q*² in the limit of zero angle. Here *q* is the scattering vector, *q* = (4π*n*/λ) sin(2θ/2), *n* being the refractive index of the solvent and λ the wavelength. The hydrodynamic radius, *R*_h, is given by the Stokes–Einstein equation, *R*_h = *k*_B*T*/(6πη*D*), *k*_B being Boltzmann's constant, *T* the absolute temperature, and η the solvent viscosity. The details of QELS instrumentation and theory are described in the literature.^{12–14}

f. Fluorescence Spectra. Fluorescence emission and excitation spectra were recorded on a Hitachi F-4500 fluorescence spectrophotometer at room temperature. Pyrene was

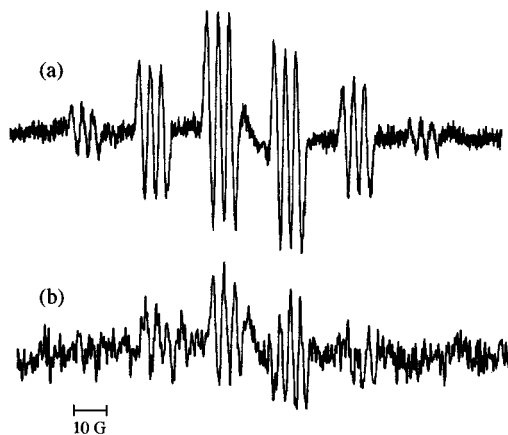


Figure 1. ESR spectra for an AzCCP solution in toluene (17 wt %) measured under irradiation of UV light at 5 °C (a) and with heating at 60 °C (b).

used as a fluorescence probe. Sample solutions were prepared by dissolving the polymer in an aqueous solution of pyrene (4.7×10^{-7} M). The pyrene stock solution was prepared as reported previously.⁶ The concentration of pyrene was determined from UV absorption at 334 nm using a molar extinction coefficient of 5.4×10^4 L/(mol cm).¹⁵ The sample solutions were properly diluted with the pyrene stock solution and sonicated for 5 min prior to measurement. For fluorescence measurements, the sample solutions were excited at 334 nm. Excitation spectra were monitored at 390 nm. Excitation and emission slit width were maintained at 5.0 and 1.0 nm, respectively.

g. Fluorescence Depolarization. Fluorescence anisotropy (r) was measured on a Hitachi F-4500 fluorescence spectrophotometer equipped with filter polarizers. Fluorescence spectra for DPH were obtained by excitation at 360 nm at 25 °C. Both excitation and emission slit width were maintained at 5.0 nm. Fluorescence anisotropy r was calculated from

$$r = \frac{I_p - I_v G}{I_p + 2I_v G} \quad (3)$$

where I_p and I_v are the fluorescence intensities measured with parallel and perpendicular orientations of the excitation and emission polarizers, respectively. G is the factor for instrumental correction. An aqueous DPH stock solution (4.0×10^{-8} M) was prepared by adding a small amount of a THF solution of DPH into pure water.^{16,17} Sample solutions were prepared by mixing the polymer with the DPH stock solution. The solutions were properly diluted with the DPH stock solution to adjust polymer concentration and sonicated for 5 min prior to measurement. The sample solutions thus prepared contain 0.14 wt % of THF. To avoid photoisomerization of DPH,¹⁸ all the sample solutions were kept in the dark.

Results

Characterization of the Polymers. ESR spectra for radicals generated from AzCCP in toluene (17 wt %) by UV irradiation at 5 °C and by heating at 60 °C are presented in Figure 1. Both the photochemically and thermally generated radicals give ESR spectra of six strong lines, each of which is split into well-resolved three lines due to coupling with a nitrogen atom. Having confirmed the radical generation from AzCCP, we performed radical polymerization of AMPS using AzCCP as an initiator at 60 °C to obtain Chol-end-capped polyAMPS (Chol-PAMPS).

Figure 2 shows ^1H NMR spectra for Chol-PAMPS measured at a polymer concentration (C_p) of 30 g/L in D_2O and in $\text{DMSO}-d_6$ at 30 °C. In D_2O , the resonance peaks due to Chol protons are not observable because of considerable line broadening, suggesting the associa-

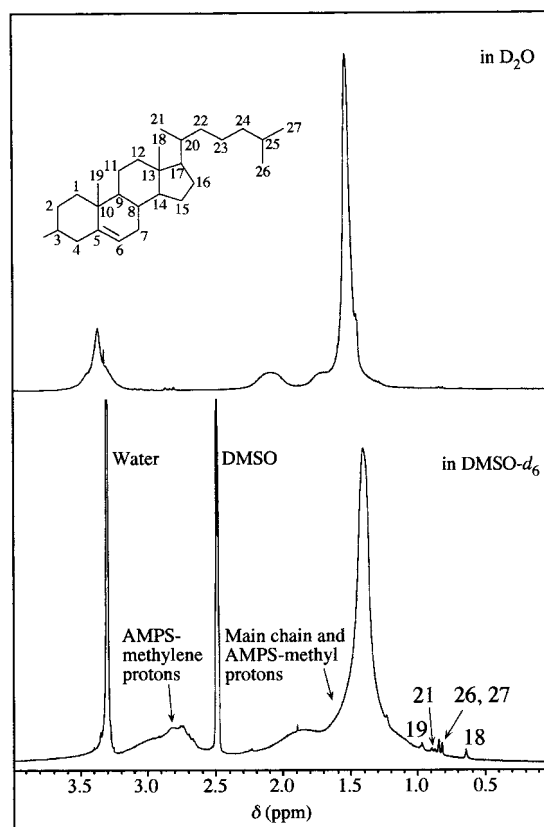


Figure 2. The 270 MHz ^1H NMR spectra of Chol-PAMPS in D_2O and in $\text{DMSO}-d_6$ at 30 °C. Assignments of the peaks are indicated by the numbers for the carbon atoms in the chemical structure of cholesterol.

tion of Chol groups. In $\text{DMSO}-d_6$, however, resonance peaks associated with the terminal Chol group are observed in the region $0.6 < \delta < 1.0$ ppm. The molar ratio of the Chol terminal group to the AMPS monomeric unit was calculated to be about 1/70 from the intensity ratio of the resonance band associated with the Chol methyl protons on C18 (see the inset in Figure 2) peaking at 0.66 ppm to the resonance band associated with the methylene protons in the AMPS side chain in the region $2.6 < \delta < 3.2$ ppm. In general, the termination of growing chain radicals in free radical polymerization occurs via either recombination or disproportionation. If we assume that all the termination of the AMPS polymerization occurs via disproportionation, the degree of polymerization (DP) of Chol-PAMPS corresponds to 70, from which the number-average molecular weight (M_n) can be calculated to be 1.36×10^4 . On the other hand, if we assume recombination, DP corresponds to 140 from which $M_n = 2.72 \times 10^4$ can be calculated.

The molecular weights of Chol-PAMPS and the reference polymer obtained by the polymerization of AMPS using AIBN as an initiator (AIBN-PAMPS) were estimated using SEC and SLS. For SEC measurements, a mixed solvent of water (0.2 M phosphate buffer, pH = 7.0) and acetonitrile (90/10, v/v) was employed as an eluent. Elution curves for Chol-PAMPS and AIBN-PAMPS are unimodal, and their molecular weights were calibrated with standard sodium poly(styrenesulfonate)s. Zimm plots for Chol-PAMPS and AIBN-PAMPS obtained by SLS measurements in 0.1 M NaCl aqueous solutions in the C_p range 5.0–20 g/L are presented in Figure 3. Chol-PAMPS yielded abnormal Zimm plots

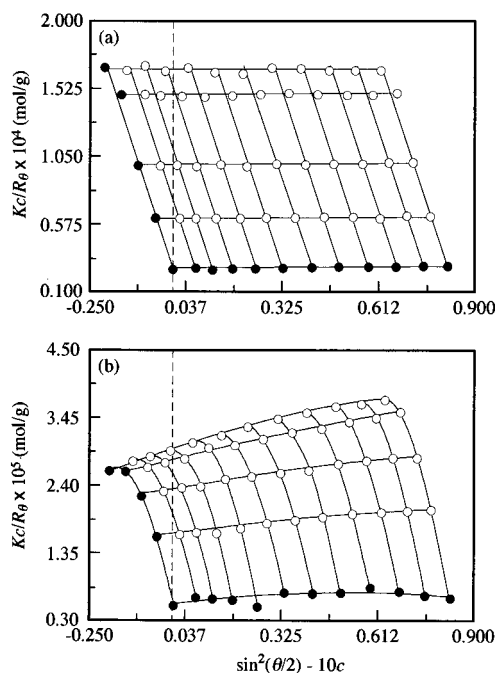


Figure 3. Zimm plots for AIBN-PAMPS (a) and Chol-PAMPS (b) in 0.1 M NaCl aqueous solution at 25 °C at angles from 30° to 130° with a 10° increment. The polymer concentration was varied from 5.0 to 20 g/L.

with a set of nonlinear lines, whereas AIBN-PAMPS showed normal Zimm plots with linear lines. For Chol-PAMPS, an apparent weight-average molecular weight (M_w) was estimated by the extrapolation of the scattering angle (θ) to zero. The molecular weights estimated by SEC and SLS for Chol-PAMPS and AIBN-PAMPS are summarized in Table 1 together with apparent mean-square radii of gyration ($\langle s^2 \rangle^{1/2}$) estimated from the slope of the angular dependence in the Zimm plots in a chosen θ range. Chol-PAMPS and AIBN-PAMPS show similar values in both M_n and M_w estimated by SEC in water/acetonitrile. However, the apparent M_w value obtained by SLS for Chol-PAMPS is more than 4 times larger than that for AIBN-PAMPS. In addition, an apparent $\langle s^2 \rangle^{1/2}$ value for Chol-PAMPS is about 4 times larger than that for AIBN-PAMPS. These observations, taken together with the motional line broadening for the Chol protons in ^1H NMR spectra in D_2O (Figure 2), indicate that the Chol-terminal groups undergo association in aqueous solutions.

The M_w values for AIBN-PAMPS obtained by SEC and SLS (3.23×10^4 and 4.00×10^4 , respectively) are fairly close to each other, suggesting that SEC under the conditions employed yields a reasonably good estimate of molecular weights for the AMPS polymers. The value of M_n estimated by SEC for Chol-PAMPS (1.45×10^4) is in fair agreement with the M_n value calculated from ^1H NMR by assuming disproportionation for the termination (1.36×10^4). The M_n value calculated by assuming recombination (2.72×10^4) is more than twice larger than the M_n value estimated by SEC. These findings suggest that the termination of the AMPS polymerization occurs mainly via disproportionation, yielding polymers possessing one Chol terminal group at one chain end.

It is known that recombination is the dominant chain terminating process in the case of styrene polymerization,¹⁹ whereas both disproportionation and recombina-

tion occur in methyl methacrylate (MMA) polymerization.²⁰ Except for these two cases, the detailed termination mechanisms for other monomers, including AMPS, are not known.

As reported by Winnik and co-workers,^{7,8,21} PNIPAM obtained by polymerization initiated with a dioctadecyl analogue of AzCCP contains the hydrophobe at only one chain end, suggesting the termination in the free radical polymerization of NIPAM occurs via disproportionation and/or chain transfer. Given the AMPS and NIPAM monomers are both acrylamides, it may be reasonable to consider that the termination processes for these two monomers are similar, assuming that the reactivities of their growing chain radicals are similar to each other.

QELS Studies. The association of the Chol terminal groups in water was confirmed by QELS measurements. Figure 4 shows relaxation time distributions for AIBN-PAMPS and Chol-PAMPS at varying measuring angles at $C_p = 10$ g/L in 0.1 M aqueous NaCl. AIBN-PAMPS exhibits unimodal distributions at any angles. However, the distributions for Chol-PAMPS are bimodal with fast and slow relaxation modes. The peaks for the fast mode show relaxation times similar to those for AIBN-PAMPS at the same scattering angles. Thus, the fast and slow mode peaks for Chol-PAMPS can be ascribed to nonassociated polymers (i.e., unimers) and multipolymer aggregates, respectively.

The relaxation rates (Γ), estimated from the QELS data at different measuring angles, are plotted as a function of the square of the scattering vector (q^2) in Figure 5. Linear relationship passing through the origin indicates that all the relaxation modes are virtually due to diffusive processes. Approximate values of the hydrodynamic radii (R_h) were calculated from the Stokes-Einstein relation along with the viscosity of water using approximate values of the diffusion coefficients (D) estimated from the slopes of the $\Gamma - q^2$ plots. Values of R_h thus obtained for AIBN-PAMPS and Chol-PAMPS are listed in Table 1. These R_h values are in good agreement with those calculated from the relaxation rates at the peak top of the relaxation time distribution in QELS at a fixed angle of 90°.

Figure 6 shows relaxation time distributions for AIBN-PAMPS and Chol-PAMPS measured at $\theta = 90^\circ$ at varying C_p in 0.1 M NaCl. AIBN-PAMPS shows unimodal distributions in the whole range of C_p examined. On the other hand, Chol-PAMPS exhibits an apparently unimodal distribution at $C_p = 0.5$ g/L with a peak relaxation time similar to that for AIBN-PAMPS. This suggests that all the Chol-PAMPS chains exist as unimers at this low polymer concentration. However, Chol-PAMPS shows bimodal distributions at higher C_p , and the area of the slow mode distribution peak relative to that of the fast mode distribution peak increases gradually as C_p is increased. These results indicate that multipolymer aggregates begin to be formed at C_p between 0.5 and 1.0 g/L, and the ratio of the aggregate relative to the unimer increases as C_p is increased in the whole range of C_p given in Figure 6.

It is to be noted here that the apparent M_w and $\langle s^2 \rangle^{1/2}$ values for Chol-PAMPS (Table 1) estimated from the Zimm plots in the C_p range 5.0–20 g/L (Figure 3) are average values for the multipolymer aggregate and the unimer. Although we cannot determine the average mass of the multipolymer aggregate separately from that of the unimer, it should be meaningful to show the much larger M_w and $\langle s^2 \rangle^{1/2}$ values for Chol-PAMPS than

Table 1. Number- and Weight-Average Molecular Weights, Radii of Gyration, and Hydrodynamic Radii

	$M_n \times 10^4$		$M_w \times 10^4$		$\langle s^2 \rangle^{1/2} \text{ }^c \text{ (nm)}$	$R_g \text{ }^d \text{ (nm)}$	
	SEC ^a	NMR ^b	SEC ^a	SLS ^c		fast ^e	slow ^f
AIBN-PAMPS	1.09		3.23	4.00	13.5	4.33	
Chol-PAMPS	1.45	1.36	3.87	17.9	55.9	4.50	65.8

^a Determined by SEC using a mixed solvent of water (0.2 M phosphate buffer, pH = 7.0) and acetonitrile (90/10, v/v) as an eluent at 45 °C. ^b Calculated from ¹H NMR spectra in DMSO-*d*₆ at 30 °C. ^c Apparent weight-average molecular weights and radii of gyration determined by SLS in 0.1 M NaCl aqueous solution at 25 °C. ^d Calculated from QELS data using the Stokes-Einstein equation at a polymer concentration of 10 g/L. ^e For the fast mode relaxation in QELS. ^f For the slow mode relaxation in QELS.

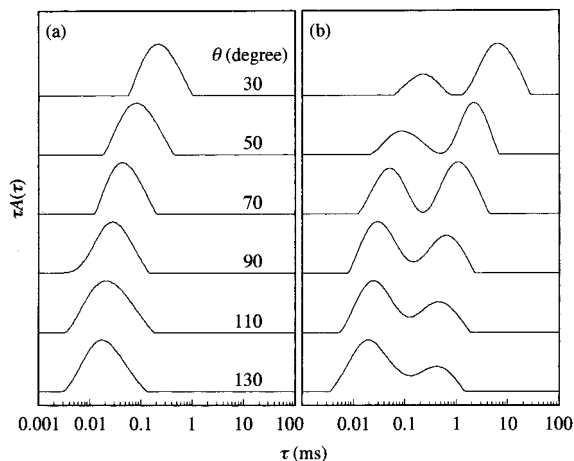


Figure 4. Distributions of the relaxation times in QELS at varying scattering angles for AIBN-PAMPS (a) and Chol-PAMPS (b) in 0.1 M NaCl aqueous solutions ($C_P = 10$ g/L) at 25 °C.

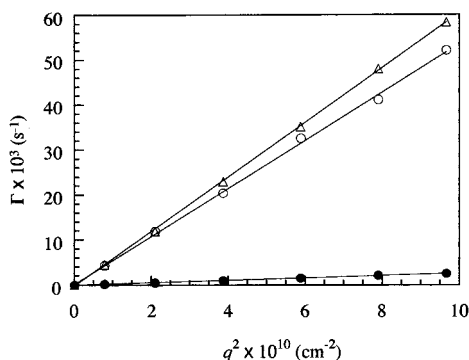


Figure 5. Relationship between Γ and q^2 for AIBN-PAMPS (Δ), the fast mode for Chol-PAMPS (○), and the slow mode for Chol-PAMPS (●) in 0.1 M NaCl aqueous solutions ($C_P = 10$ g/L) at 25 °C.

those for AIBN-PAMPS as a qualitative indication of the presence of the multipolymer aggregates in Chol-PAMPS in water.

In Figure 7, R_h values calculated from the relaxation rates at the peak top of the relaxation time distribution at $\theta = 90^\circ$ were plotted against C_P . The R_h values for the slow mode for Chol-PAMPS are nearly constant in the C_P regime $1.0 < C_P < 5.0$ g/L, but R_h increases significantly when C_P is increased beyond this C_P regime. These observations indicate that the number of Chol-PAMPS chains involved in one multipolymer aggregate increases significantly with C_P when $C_P > 5.0$ g/L. On the other hand, the relaxation time for the fast mode shows a tendency similar to that for the reference polymer; that is, the relaxation time decreases slightly with an increase in C_P , a normal tendency for simple polyelectrolytes. This is an indication of the presence of unimers coexisting with the aggregates in the whole range of C_P studied.

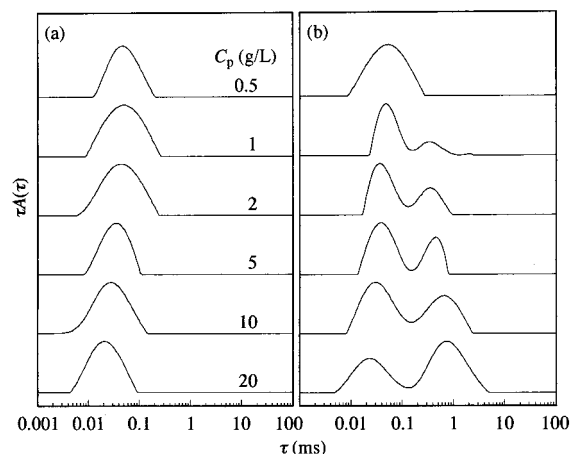


Figure 6. Distributions of the relaxation times in QELS at $\theta = 90^\circ$ for AIBN-PAMPS (a) and Chol-PAMPS (b) in 0.1 M NaCl aqueous solutions at varying C_P at 25 °C.

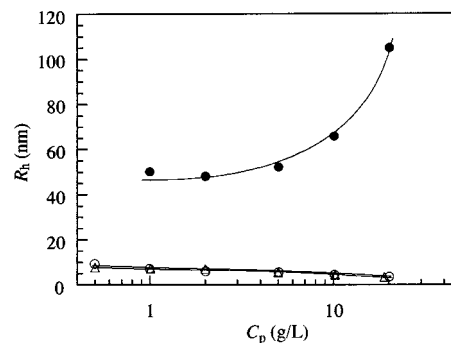


Figure 7. Plots of R_h for AIBN-PAMPS (Δ), the fast mode for Chol-PAMPS (○), and the slow mode for Chol-PAMPS (●) as a function of C_P in 0.1 M NaCl aqueous solutions at $\theta = 90^\circ$ at 25 °C.

Fluorescence Studies. Pyrene is commonly used as a fluorescence probe to monitor micropolarity^{22,23} because the ratio of the third to the first vibronic peaks (I_3/I_1) in pyrene fluorescence spectra is sensitive to the polarity,²⁴ the I_3/I_1 ratio being larger in less polar media. Figure 8 compares fluorescence spectra for pyrene solubilized in aqueous solutions ($C_P = 10$ g/L) of AIBN-PAMPS and Chol-PAMPS. The I_3/I_1 ratios in the presence of AIBN-PAMPS and Chol-PAMPS are estimated to be 0.55 and 0.86, respectively. The I_3/I_1 ratio for pyrene solubilized in sodium dodecyl sulfate (SDS) micelle in water is 0.88,²⁴ whereas the ratio in pure water is 0.54. Therefore, we can conclude that in the Chol-PAMPS solution pyrene probes are solubilized in hydrophobic microdomains formed by the terminal Chol groups, whereas in the AIBN-PAMPS solution, the probe experiences the polarity of bulk water.

The association of the terminal Chol groups leads to the formation of hydrophobic microdomains. In Figure

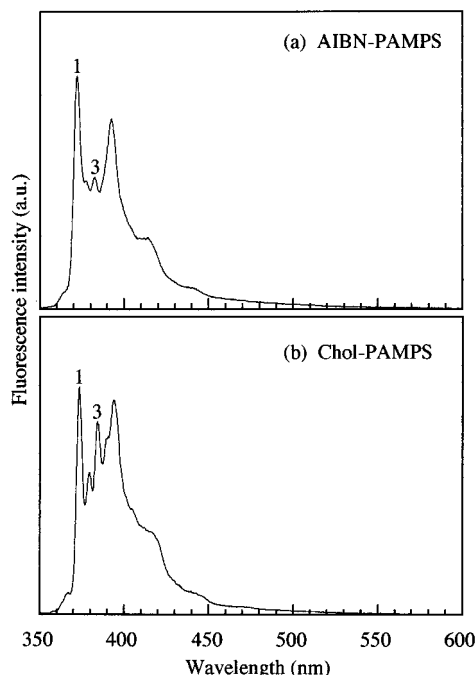


Figure 8. Fluorescence spectra for pyrene probes in the presence of 10 g/L of AIBN-PAMPS (a) and Chol-PAMPS (b) in aqueous solution (excitation wavelength, 334 nm).

9a, the I_3/I_1 ratios for AIBN-PAMPS and Chol-PAMPS in water are plotted as a function of C_p . The I_3/I_1 ratios for AIBN-PAMPS are constant at 0.54–0.55, independent of C_p over the whole range of C_p examined, pyrene experiencing the polarity of bulk water. In the case of Chol-PAMPS, the I_3/I_1 ratios are practically constant at 0.54 in a lower C_p region, but the ratio begins to increase at $C_p > 0.1$ g/L with increasing C_p , reaching a large value of about 0.87 at $C_p = 20$ g/L. This large I_3/I_1 value may be an indication that hydrophobic microdomains formed by the self-aggregation of the Chol end groups are as hydrophobic as the interior of SDS micelles. These observations may suggest the presence of a specific C_p at which a micellelike structure begins to be formed by Chol-PAMPS (i.e., the critical micelle concentration (cmc) for Chol-PAMPS) upon an increase in C_p .

It is established that a cmc for surfactant molecules can be determined by the I_{338}/I_{333} ratio for the (0–0) band in pyrene excitation spectra, where I_{333} and I_{338} are the pyrene fluorescence intensities excited at 333 and 338 nm, respectively.²⁵ In Figure 9a, the I_{338}/I_{333} ratios are plotted as a function of C_p . The I_{338}/I_{333} ratio for AIBN-PAMPS shows a value characteristic of pyrene in water over the whole range of C_p studied. In the case of Chol-PAMPS, however, the I_{338}/I_{333} ratio increases with increasing C_p over a range of $0.1 < C_p < 20$ g/L. The apparent cmc may be determined graphically to be about 0.6 g/L. Since the I_3/I_1 ratio changes parallel with the I_{338}/I_{333} ratio as can be seen in Figure 9a, the cmc for Chol-PAMPS may also be estimated graphically from the I_3/I_1 ratio. It is to be noted, however, that a change in the I_3/I_1 ratio for Chol-PAMPS occurs over a wide range of polymer concentrations (i.e., $0.1 < C_p < 20$ g/L). Similar observations of a broad transition have been reported by Winnik and co-workers⁷ for the aggregation of hydrophobically end-alkylated PNIPAM and by Almgren et al.⁹ for the aggregation of poly(ethylene oxide) carrying two alkyl end groups of 12 carbon atoms.

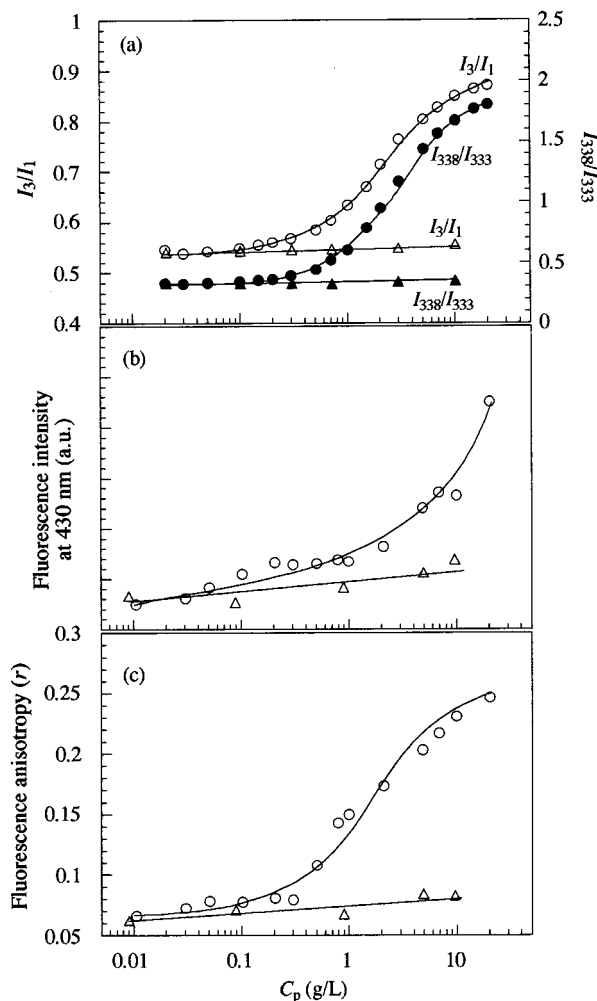


Figure 9. (a) Plots of the I_3/I_1 and I_{338}/I_{333} ratios in pyrene fluorescence emission and excitation spectra, respectively, as a function of C_p for AIBN-PAMPS (triangles) and Chol-PAMPS (circles) in aqueous solutions (excitation wavelength, 334 nm; emission wavelength, 390 nm). (b) Intensity of DPH fluorescence at 430 nm in aqueous solution (containing 0.14 wt % of THF) as a function of C_p for AIBN-PAMPS (Δ) and Chol-PAMPS (\circ) at 25 °C. (c) Fluorescence anisotropy (r) for DPH as a function of C_p for AIBN-PAMPS (Δ) and Chol-PAMPS (\circ) (excitation wavelength, 430 nm; emission wavelength, 360 nm).

1,6-Diphenyl-1,3,5-hexatriene (DPH) is a useful fluorescence probe for studies of structures and dynamic properties of membranes.²⁶ In Figure 9b, the intensities of DPH fluorescence in aqueous solutions of Chol-PAMPS and AIBN-PAMPS are plotted as a function of C_p . In the Chol-PAMPS solution, the fluorescence intensity increases considerably with an increase in C_p , whereas in the AIBN-PAMPS solution, it increases only slightly. These observations imply that DPH probes are solubilized in hydrophobic microdomains formed from the Chol end groups of Chol-PAMPS. When DPH probes are solubilized in the hydrophobic microdomains, rotational motions of the probe may be restricted. To monitor the mobility of the probe, the fluorescence anisotropy (r) was measured at an emission maximum of 430 nm at 25 °C. Figure 9c shows plots of r as a function of C_p for Chol-PAMPS and AIBN-PAMPS. A rather abrupt increase in r was observed for Chol-PAMPS at a C_p near 0.4 g/L, the tendency being fairly close to those observed for the I_3/I_1 and I_{338}/I_{333} ratios (Figure 9a). It should be noted that in the region $C_p <$

5.0 g/L the DPH fluorescence intensity in Figure 9b increases with C_P more gradually than r in Figure 9c. These observations suggest that the onset of an increase in r corresponds to the onset of the micellelike aggregate formation whereas the increase in the fluorescence intensity in Figure 9b reflects an increment of the number of the micellelike aggregates with an increase in C_P . This is probably because the partition coefficient for DPH in the micellelike aggregate is very low.

Discussion

On the basis of the finding that DP estimated from ^1H NMR assuming each polymer chain has one Chol end group agreed fairly well with DP estimated from SEC, we assumed disproportionation as a main chain termination reaction. However, we cannot rule out the possibility that polymer chains possessing one Chol group per chain are produced not only via disproportionation but also via chain transfer to the solvent. If the chain transfer occurs along with recombination for the substantial chain termination, then polymer chains could appear to have only one Chol group per chain on average. If this is the case, the polymerization product is a mixture of polymer chains possessing no Chol group, only one Chol at one chain end, and two Chol groups at both ends.

It is expected that Chol-PAMPS having a Chol group at one chain end would form a spherical core-corona type micelle with a Chol aggregate in the core and polyAMPS chains in the corona. In such a case, R_h of the micelle should be equal to or smaller than the length of fully extended Chol-PAMPS chain. For Chol-PAMPS of DP = 70, this length is approximately 20 nm. However, R_h values observed by QELS in the C_P regime of 1.0–5.0 g/L are on the order of 50 nm. This size is obviously too large for a single core-corona micelle. Furthermore, when C_P is increased beyond this C_P regime, R_h further increases with increasing C_P . For instance, R_h increases to 105 nm at $C_P = 20$ g/L. This is highly unlikely for spherical core-corona type micelles.

Winnik and co-workers⁷ reported that end-di-octadecylated PNIPAM of DP = 280–540 formed spherical micelles with octadecyl groups in the core and PNIPAM chains in the corona, and their effective diameters were on the order of 70 nm at 20 °C. Their end-di-octadecylated PNIPAM samples have much larger DP than that of Chol-PAMPS, but the sizes of their micelles are smaller than those formed from Chol-PAMPS.

These findings suggest that some polymer chains possess two Chol groups at both chain ends. Namely, even if most polymers have one Chol group at one chain end and they form spherical micelles as expected, a small number of polymers possessing Chol groups at both ends can bridge the micelles. This is because the Chol groups at the ends of the same polymer chain can occupy different micelles. The micelle bridging by such polymers causes an increase in the hydrodynamic size. Moreover, the micelle bridging should occur to a larger extent at higher polymer concentrations, thus leading to a large increase in R_h with increasing polymer concentration, as observed in Figure 7.

The micelles are formed only at polymer concentrations higher than a cmc (Figure 9). Furthermore, the micelles coexist with unimers and the micelle/unimer ratio increases with increasing polymer concentration (Figure 6). These findings suggest that the unimers are

mainly, if not all, polymer chains possessing a Chol group (or two Chol groups) per chain and not polymers having no Chol group. The results in Figures 6 and 9 suggest that the micelles are formed in an equilibrium process.

Conclusions

Chol-PAMPS, polyAMPS possessing a Chol moiety at chain end, was prepared by free radical polymerization of AMPS using AzCCP as an initiator, and the associative behavior of Chol-PAMPS in aqueous solutions was investigated by ^1H NMR, SEC, SLS, QELS, and fluorescence probe techniques. AIBN-PAMPS, polyAMPS prepared in the presence of AIBN as an initiator, was used as a reference polymer. The degree of polymerization of Chol-PAMPS was estimated to be about 70 based on an ^1H NMR spectrum measured in DMSO- d_6 by assuming the chain termination to occur via disproportionation. This DP value agreed fairly well with that estimated by SEC in water/acetonitrile (90/10, v/v). M_w values of Chol-PAMPS and AIBN-PAMPS, estimated by SEC, were similar. AIBN-PAMPS in 0.1 M NaCl gave a Zimm plot with a set of linear lines in the C_P regime of 5.0–20 g/L, but, in contrast, Chol-PAMPS yielded a considerably curved Zimm plot under the same conditions. An apparent M_w ($=17.9 \times 10^4$) value for Chol-PAMPS, roughly estimated from the curved Zimm plot, was more than 4 times larger than M_w ($=4.00 \times 10^4$) of AIBN-PAMPS, indicating a tendency of Chol-PAMPS for self-association. QELS data indicated that the self-association of Chol-PAMPS occurred when $C_P > 0.5$ g/L. Fluorescence emission and excitation spectra for pyrene probes solubilized in the aggregates of Chol-PAMPS suggested the presence of the cmc around $C_P \approx 0.6$ g/L in water. Above the cmc, the micellelike aggregates coexist with unimers over a wide range of C_P (e.g., even at $C_P \approx 20$ g/L). In the C_P regime of 1.0–5.0 g/L, R_h for the aggregate was nearly constant at about 50 nm, but when C_P is increased beyond this C_P regime, R_h increased with increasing C_P . Considering that DP ≈ 70 for Chol-PAMPS, the sizes observed for the aggregates are obviously too large for a single spherical micelle with Chol groups in the core and extended polyAMPS chains in the corona. However, these results are explained by considering that there are some polymer chains possessing Chol groups at both chain ends (formed via recombination) and that spherical micelles are bridged by these polymer chains.

Acknowledgment. This work was supported in part by a Grant-in-Aid for Scientific Research No. 10450354 from the Ministry of Education, Science, Sports, and Culture, Japan.

References and Notes

- (1) Demel, R. A.; De Kruffy, B. *Biochim. Biophys. Acta* **1976**, *457*, 109–132.
- (2) Akiyoshi, K.; Deguchi, S.; Moriguchi, N.; Yamaguchi, S.; Sunamoto, J. *Macromolecules* **1993**, *26*, 3062–3068.
- (3) Nishikawa, T.; Akiyoshi, K.; Sunamoto, J. *Macromolecules* **1994**, *27*, 7654–7659.
- (4) Akiyoshi, K.; Deguchi, S.; Tajima, H.; Nishikawa, T.; Sunamoto, J. *Macromolecules* **1997**, *30*, 857–861.
- (5) Nishikawa, T.; Akiyoshi, K.; Sunamoto, J. *J. Am. Chem. Soc.* **1996**, *118*, 6110–6115.
- (6) Yusa, S.; Kamachi, M.; Morishima, Y. *Langmuir* **1998**, *14*, 6059–6067.
- (7) Winnik, F. M.; Davidson, A. R.; Hamer, G. K.; Kitano, H. *Macromolecules* **1992**, *25*, 1876–1880.

- (8) Yamazaki, A.; Song, J. M.; Winnik, F. M.; Brash, J. L. *Macromolecules* **1998**, *31*, 109–115.
- (9) Alami, E.; Almgren, M.; Brown, W.; François, J. *Macromolecules* **1996**, *29*, 2229–2243.
- (10) Jakes, J. *Czech. J. Phys.* **1988**, *B38*, 1305–1316.
- (11) Stockmayer, W. H.; Schmidt, M. *Pure Appl. Chem.* **1982**, *54*, 407–414.
- (12) Phillies, G. D. J. *Anal. Chem.* **1990**, *62*, 1049A–1057A.
- (13) Phillies, G. D. J. *J. Chem. Phys.* **1988**, *89*, 91–99.
- (14) Koppel, D. E. *J. Chem. Phys.* **1972**, *57*, 4814–4820.
- (15) Berlman, I. B. *Handbook of Fluorescence Spectra of Aromatic Molecules*; Academic Press: New York, 1971.
- (16) Andrich, M. P.; Vanderkooi, J. M. *Biochemistry* **1976**, *15*, 1257–1261.
- (17) Johnson, S. M.; Nicolau, C. *Biochem. Biophys. Res. Commun.* **1977**, *76*, 869–874.
- (18) Saltiel, J.; Ko, D. H.; Fleming, S. A. *J. Am. Chem. Soc.* **1994**, *116*, 4099–4100.
- (19) Mayo, F. R.; Gregg, R. A.; Matheson, M. S. *J. Am. Chem. Soc.* **1951**, *73*, 1691–1700.
- (20) Alfrey, T., Jr.; Price, C. C. *J. Polym. Sci.* **1947**, *2*, 101–106.
- (21) Winnik, F. M.; Adronov, A.; Kitano, H. *Can. J. Chem.* **1995**, *73*, 2030–2040.
- (22) Procházka, K.; Martin, T. J.; Munk, P.; Webber, S. E. *Macromolecules* **1996**, *29*, 6518–6525.
- (23) Lianos, P.; Viriot, M. L.; Zana, R. *J. Phys. Chem.* **1984**, *88*, 1098–1101.
- (24) Kalyanasundaram, K.; Thomas, J. K. *J. Am. Chem. Soc.* **1977**, *99*, 2039–2044.
- (25) Wilhelm, M.; Zhao, C.-L.; Wang, Y.; Xu, R.; Winnik, M. A.; Mura, J.-L.; Riess, G.; Croucher, M. D. *Macromolecules* **1991**, *24*, 1033–1040.
- (26) Shinitzky, M.; Barenholz, Y. *J. Biol. Chem.* **1974**, *249*, 2652–2657.

MA990802I